



# Development of a hybrid adsorbent for CO<sub>2</sub> capture by the physical mixture of Na-ZSM-5 zeolite and activated carbon

Jorge Arce Castro<sup>1,2</sup>, Lourdes Oliveira Galvão<sup>1,2</sup>, Yanier Sánchez Hechavarria<sup>2</sup>, Tamille Alves Souza<sup>2,3</sup>, Karen Pontes Valverde<sup>1,3</sup>, Mauricio Brandão dos Santos<sup>1,2</sup>, Fernanda Teixeira Cruz<sup>1,2</sup>, Raildo Alves Fiuza Junior<sup>1,2,4</sup>, Artur José Santos Mascarenhas<sup>1,2,4,\*</sup>

#### Resumo / Abstract

RESUMO – Neste trabalho, foram desenvolvidos materiais híbridos para captura de CO<sub>2</sub> via adsorção por variação de temperatura (TSA). Estes híbridos foram produzidos pela mistura física de carvão ativado obtido de caroços de cajá e do zeólito Na-ZSM-5 sintetizado por uma rota sustentável, em três composições distintas. Os materiais foram caracterizados por MEV, DRX, TG e análise textural. A avaliação da adsorção de CO<sub>2</sub> foi realizada por análise termogravimétrica. O adsorvente híbrido H-30Z/70AC (30% zeólito/70% carvão ativado) exibiu o melhor desempenho, com uma capacidade de adsorção de 71,67 mg g<sup>-1</sup>. Adicionalmente, a seletividade CO<sub>2</sub>/N<sub>2</sub> a 1 bar e 30°C foi investigada, obtendo valores de 4,6 para H-70Z/30AC e H-50Z/50AC e 5,0 para o adsorvente H-30Z/70AC, respectivamente, considerando uma vazão de 100 mL min<sup>-1</sup> de uma mistura gasosa de CO<sub>2</sub>:N<sub>2</sub> na proporção de 1:1.

Palavras-chaves: Materiais híbridos, Adsorção de CO2, TSA, mistura física

ABSTRACT - In this work, hybrid materials were developed for CO<sub>2</sub> capture via temperature swing adsorption (TSA). These hybrids were produced by physically mixing activated carbon obtained from yellow mombin seeds and Na-ZSM-5 zeolite synthesized through a sustainable route (in three distinct compositions). SEM, XRD, TGA, and textural analysis characterized the materials. The evaluation of CO<sub>2</sub> adsorption was performed by thermogravimetric analysis. The H-30Z/70AC hybrid adsorbent (30% zeolite/70% activated carbon) exhibited the best performance, with an adsorption capacity of 71.67 mg g<sup>-1</sup>. Additionally, the CO<sub>2</sub>/N<sub>2</sub> selectivity was investigated at 1 bar and 30°C, obtaining values of 4.6 for both H-70Z/30AC and H-50Z/50AC and 5.0 for H-30Z/70AC adsorbents, respectively, considering a flow rate of 100 mL min<sup>-1</sup> of a gas mixture of CO<sub>2</sub>:N<sub>2</sub> in a 1:1 ratio.

**Keywords**: Hybrid materials, CO<sub>2</sub> adsorption, TSA, physical mixture

### Introduction

The increasing concentration of  $CO_2$  in the atmosphere has been recognized as the main contributor to global warming (1-2). This, in combination with the growing global demand for energy, represents an urgent challenge in mitigating climate change (3-4). In response to this problem, the development of new promising materials for the capture of polluting gases such as  $CO_2$  and NOx has received considerable attention (5). In this context, a variety of solid physical adsorbents have been investigated for this purpose, including microporous and mesoporous carbon-

based structures, such as activated carbon (AC) and carbon molecular sieves, mesoporous siliceous materials, zeolites, metal-organic frameworks (MOFs), metal oxides, and others (6-9).

The development of a new generation of hybrid adsorbents (HAs) for CO<sub>2</sub> capture, through the confinement of amines in solid supports, has been a central focus in current research. In these systems, a strong amine-CO<sub>2</sub> interaction, similar to conventional absorption, is expected (10). Meanwhile, the development of HAs from the physical mixture of synthesized zeolites and activated carbons obtained from biomass has been underexplored.

<sup>&</sup>lt;sup>1</sup>Programa de Pós-Graduação em Energia e Ambiente (PGENAM), Escola Politécnica, Universidade Federal da Bahia, R. Prof Aristides Novis, 2, Federação, 40120-910, Salvador - BA.

<sup>&</sup>lt;sup>2</sup>Laboratório de Catálise e Materiais (LABCAT), Departamento de Química Geral e Inorgânica, Instituto de Química, Universidade Federal da Bahia, Travessa Barão de Jeremoabo, 147, Campus Ondina, 40170-280, Salvador - BA.

<sup>&</sup>lt;sup>3</sup>Laboratório de Processos e Energias Sustentáveis (LAPSER), Escola Politécnica, Universidade Federal da Bahia, R. Aristides Novis, 2 Federação, 40210-630, Salvador – BA.

<sup>&</sup>lt;sup>4</sup> Programa de Pós-graduação em Química, Instituto de Química, Universidade Federal da Bahia, Travessa Barão de Jeremoabo, 147, Campus Ondina, 40170-280, Salvador - BA.

<sup>\*</sup> e-mail: artur@ufba.br



HAs based on mixtures of zeolites and activated carbons are frequently employed in electric swing adsorption (ESA) processes, a variant of temperature swing adsorption (TSA) where electric energy is used to heat the adsorbent and promote CO<sub>2</sub> desorption. In the ESA process, HAs that are commonly employed are obtained from mixtures of zeolites and phenolic resin, followed by calcination to generate the

activated carbon (11 - 12).

Temperature Swing Adsorption (TSA) is a process that utilizes the periodic variation of temperature in an adsorbent bed. Adsorption occurs at low temperatures, and bed regeneration takes place at high temperatures (13). However, TSA processes generally have long cycles and are disadvantageous due to high energy consumption and the need for large stocks of adsorbents (14). In the electrical swing adsorption (ESA) process, heat generated by the Joule effect is used to regenerate the adsorbent materials, allowing precise and rapid control of the heating rate. This feature enables accelerated heating, which contributes to a more compact design of the ESA system (15).

Despite the significant potential of HAs made from physical mixtures of zeolites and microporous carbons in various adsorption techniques, industrial zeolites and activated carbons predominate in most research. Pereira et al. (6) evaluated a physical mixture of commercial activated carbon and zeolite for CO<sub>2</sub> adsorption via ESA, while Erdogan (16) synthesized an activated carbon from *Elaeagnus* stones and modified a commercial zeolite to obtain a hybrid adsorbent (HA) for CO<sub>2</sub> adsorption via PSA.

In this work, three compositions of HAs are obtained from the physical mixture of an activated carbon derived from biomass and a ZSM-5 zeolite synthesized via a sustainable route through interzeolite transformation from zeolite Y (17). Notably, this synthesis method eliminates the use of organic structure-directing agents (OSDAs), resulting in lower environmental impact without generation of CO<sub>2</sub>, reduced synthesis cost, simplified post-synthesis treatment. These advantages make the process particularly suitable for large-scale and environmentally responsible applications, in which organic structure directing agents were not used. These three hybrid materials were evaluated for CO<sub>2</sub> capture through the temperature swing adsorption (TSA) process.

## **Experimental**

Preparation of the hybrid adsorbents (HAs)

For the sustainable synthesis of Na-ZSM-5 zeolite via interzeolitic transformation from zeolite Y without using OSDAs, the method of dos Santos (17) was followed with some modifications. 3.8 g of the starting zeolite, in the acid form of zeolite Y (H-Y), was used, along with 2.04 g of NaOH in 92 mL of H<sub>2</sub>O under stirring. Subsequently, 2.04 g of NaOH was added to maintain the NaOH/SiO<sub>2</sub> ratio at 0.3, followed by the addition of 9.8572 g of Aerosil 200 silica (Synth). The mixture was kept under stirring (300 rpm) for 30 min at room temperature. The gel was



transferred to PTFE cups (previously decontaminated by at least 48 h in HF 40%), which were conditioned in stainless-steel autoclave for hydrothermal treatment for 5 days at  $150^{\circ}$ C. After the synthesis time, the autoclave was cooled, and the solid was recovered by vacuum filtration, washed with deionized water until pH = 7, and dried at  $100^{\circ}$ C.

The activated carbon was obtained from yellow mombin seeds using a two-step route. Immediately after collecting, the seeds were washed and dried for three days at a temperature of 105°C, ground in a knife mill, and subsequently, the biomass was sieved using a 100-mesh sieve. In the first step, the biomass was pyrolyzed in a vertical furnace at 400°C under a nitrogen atmosphere with a nitrogen flow rate of 150 mL min<sup>-1</sup> and a heating rate of 10°C min<sup>-1</sup>, and then impregnated with KOH in an aqueous solution at a mass ratio of 1:1. In the second step, the impregnated material was pyrolyzed at 750°C under an inert atmosphere with a nitrogen flow rate of 150 mL min<sup>-1</sup> and a heating rate of 10°C min<sup>-1</sup>. Finally, the activated carbon was washed with hydrochloric acid and distilled water until a pH value of approximately 7.0 was achieved. After washing, the carbon was dried in an oven at 100°C for 24 hours. The activated carbon was identified as AC-YMS.

From the synthesized zeolite and activated carbon, three HAs materials were prepared by physically mixing these materials in the following proportions: 70% zeolite - 30% carbon, 50% zeolite - 50% carbon, and 30% zeolite - 70% carbon. These were identified as H-70Z/30AC, H-50Z/50AC, and H-30Z/70AC, respectively.

To obtain these materials, the zeolite and the carbon, in the previously mentioned proportions, were first manually mixed in a beaker. Then, the mixture was placed in 100 mL of deionized water and vigorously stirred for one hour. The resulting paste was dried at 100°C for 36 h.

### Characterization of the adsorbents

The adsorbents were characterized by powder X-ray diffraction (XRD) in a Shimadzu XRD-6000, operating with CuK $\alpha$  radiation operating with CuK $\alpha$  radiation generated at 40 kV and 30 mA, equipped with a graphite monochromator, in the 2 $\theta$  range of 5° to 80°, with a scan rate of 2°·min<sup>-1</sup>. The thermal stability of the adsorbents was determined by thermogravimetric analysis (TGA) in an equipment Shimadzu DTG-60H, with a temperature range from 25 to 1000°C and a heating rate of 10°C·min<sup>-1</sup>, under a nitrogen flow of 50 mL·min<sup>-1</sup>. The morphology of the adsorbents was analyzed by scanning electron microscopy (SEM) in a Hitachi S-3400N microscope; the samples were dispersed on carbon tapes, without previous metallization.

#### CO<sub>2</sub> adsorption study

Adsorption studies were carried out using a Shimadzu DTG-60H thermogravimetric analysis (TGA) instrument. Cyclic adsorption studies were carried out following these steps: (i) Drying the material at 200°C for 30 min under a nitrogen flow (100 mL min<sup>-1</sup>) to remove moisture and



adsorbed gases; (ii) The adsorbent was cooled to  $30^{\circ}$ C under a nitrogen flow ( $100 \text{ mL min}^{-1}$ ); (iii) Then, a gas mixture of  $CO_2:N_2$  in a 1:1 ratio was introduced with a total flow rate of  $100 \text{ mL min}^{-1}$  for 30 min; and (iv) The gas was switched back to  $N_2$ , at a flow rate of  $100 \text{ mL min}^{-1}$ , and the sample was heated to  $150^{\circ}$ C for 15 min for desorption.

The CO<sub>2</sub> adsorption capacity (Q<sub>CO2</sub>) of the HAs in mg g<sup>-1</sup> was calculated using Equation 1:

$$Q_{CO2} = \left[ \frac{m_{ADS,F} - m_{ADS,I}}{m_{ADS,IF}} \right]$$
 (1)

where m<sub>ADS.F</sub> is the final mass of CO<sub>2</sub> adsorption and m<sub>ADS.I</sub> is the initial mass just before CO<sub>2</sub> adsorption, based on the mass gain curves of the materials.

## **Results and Discussion**

The XRD patterns of AC-YMS, shown in Figure 1, exhibits two broad amorphous halos centered at 23.5° and 43.4°, corresponding to the (002) and (100) planes of amorphous graphitic carbon. This characteristic reveals a material with a predominantly amorphous structure and disordered graphitic planes (18). The observation of a shift in the (002) reflection peak to a diffraction angle of 23.5°, when compared to the 26.3° of graphite, suggests an increase in the interlayer spacing in the activated carbon. The increase in interlayer spacing can impact properties such as adsorption, chemical reactivity, and electrical conductivity.

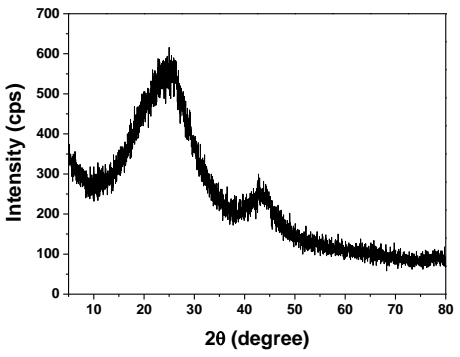


**Figure 1**. X-ray diffraction patterns of the activated carbon derived from yellow mombin seeds (AC-YMS).

Figure 2 presents the XRD patterns of the Na-ZSM-5 zeolite and the adsorbents H-70Z/30AC, H-50Z/50AC, and H-30Z/70AC. The diffractogram of the Na-ZSM-5 zeolite reveals a typical profile of the MFI topology, indicating high crystallinity, a result that agrees with those reported by dos Santos (17). The addition of AC-YMS activated carbon significantly altered the diffraction patterns of the zeolite in the HAs, as illustrated in the Figure 2. These materials exhibit a crystalline profile with the characteristic peaks of the zeolite crystalline structure, a result of the synthesis method used, having a greater impact on H-30Z/70AC,



which corresponds to the expected results given that activated carbon has an amorphous structure.

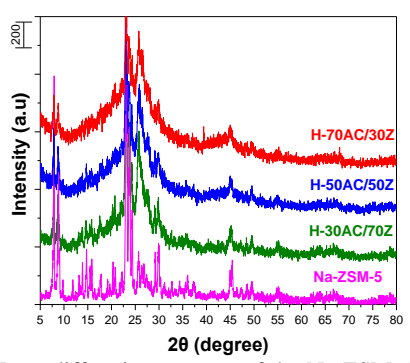


**Figure 2.** X-ray diffraction patterns of the Na-ZSM-5 zeolite and the HAs obtained from physical mixture with activated carbon.

The SEM images of the activated carbon, zeolite, and HAs are illustrated in Figure 3.

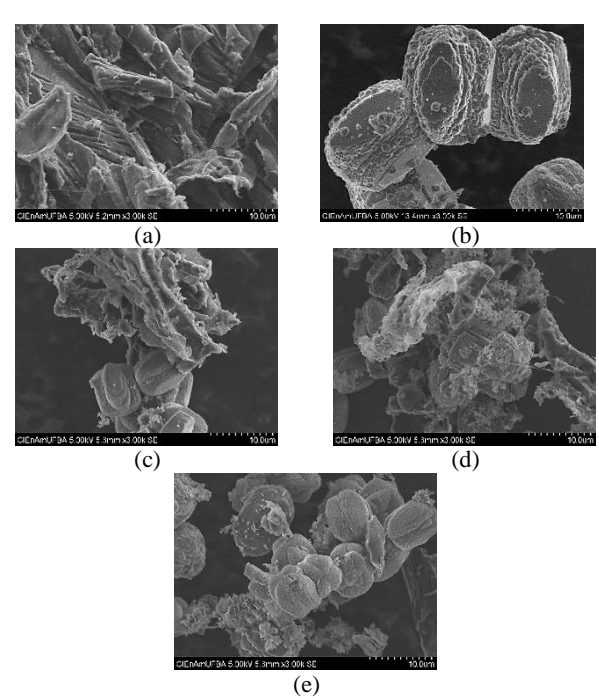


**Figure 3.** Scanning electron microscopy of the adsorbents: (a) AC-YMS; (b) Na-ZSM-5; (c) H-50Z/50AC; (d) H-70Z/30AC; (e) H-30Z/70AC.

In Figure 3.a, it is observed that AC-YMS exhibits a rough surface, which may originate from the lignocellulosic biomass structure from which it was obtained, but also by the KOH activation process. According to Heidarinejad et al. (19), KOH decomposition during pyrolysis produces potassium oxide and water, that can react with carbon walls, originating gases such as H<sub>2</sub>, H<sub>2</sub>O, CO and CO<sub>2</sub>. Besides, KOH react with carbon walls, producing metallic potassium, hydrogen and K<sub>2</sub>CO<sub>3</sub>. Metallic potassium can migrate into carbon walls by structure intercalation, leading



to the expansion of existing pores and the creation of new ones.

In Figure 3.b, it can be observed that Na-ZSM-5 presents aggregates in the form of plates forming hexagonal polyhedron, characteristic of the crystallites of the ZSM-5 zeolite morphology with MFI topology (17). The morphology of the H-50Z/50AC adsorbent shown in Figure 3.c reveals Na-ZSM-5 crystals dispersed in the activated carbon. The SEM micrograph of the H-70Z/30AC adsorbent (Figure 3.d) reveals a heterogeneous distribution of abundant activated carbon around the ZSM-5 crystals. In contrast, the image of the H-30Z/70AC adsorbent (Figure 3.f) exhibits a higher concentration of hexagonal polyhedral crystals characteristic of Na-ZSM-5, with small amounts of activated carbon dispersed around them.

The results of the textural analysis of the adsorbents are presented in Figures 4 and in Table 1.

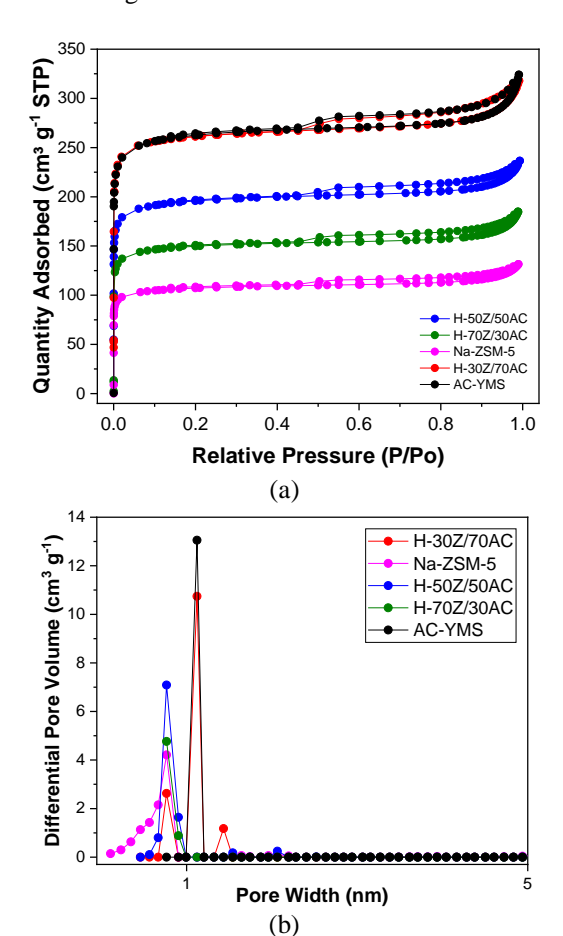


Figure 4. (a)  $N_2$  physisorption isotherms; and (b) NLDFT pore size distribution of the precursor's materials and HAs.

Figure 4.a shows the nitrogen (N<sub>2</sub>) physisorption isotherms of the activated carbon AC-YMS, Na-ZSM-5 zeolite and HAs. According to the IUPAC classification (20), the AC-YMS and the adsorbents H-30Z/70AC exhibited a type I(a) adsorption isotherm, common in microporous materials, showing a type H4 hysteresis loop at



 $P/P_0 \approx 0.4$ , typical of microporous materials with the presence of small mesopores (7).

The pore size distribution obtained by NLDFT is shown in the Figure 4.b and Table 1. It can be observed that both the precursor materials and the activated hybrids (HAs) are predominantly microporous. Among them, AC-YMS ( $S_{micro}=1151\ m^2\ g^{-1};\ V_{micro}=0.365\ cm^3\ g^{-1})$  and H-30Z/70AC ( $S_{micro}=861\ m^2\ g^{-1};\ V_{micro}=0.364\ cm^3\ g^{-1})$  stand out, exhibiting the highest specific surface areas and micropore volumes.

**Table 1.** Textural properties of the precursors and HAs.

Sample	$^{a}S_{BET}$ $(m^{2} g^{-1})$	<sup>b</sup> S <sub>micro</sub> (m <sup>2</sup> g- <sup>1</sup> )	cV <sub>micro</sub> (cm <sup>3</sup> g <sup>-1</sup> )	cV <sub>meso</sub> (cm <sup>3</sup> g <sup>-1</sup> )
Na-ZSM-5	356	461	0.219	0.074
AC-YMS	925	1151	0.365	0.034
H-30Z/70AC	693	861	0.364	0.042
H-50Z/50AC	530	658	0.281	0.026
H-70Z/30AC	379	470	0.267	0.038

<sup>&</sup>lt;sup>a</sup>S<sub>BET</sub>, surface area calculated by BET equation at P/P<sub>0</sub>= 0.05–0.2;

The thermal stability of the materials AC-YMS, Na-ZSM-5, the hybrid adsorbents (H-30Z/70AC, H-50Z/50AC and H-70Z/30AC) was evaluated by thermogravimetric analysis (TGA), as illustrated in Figure 5.

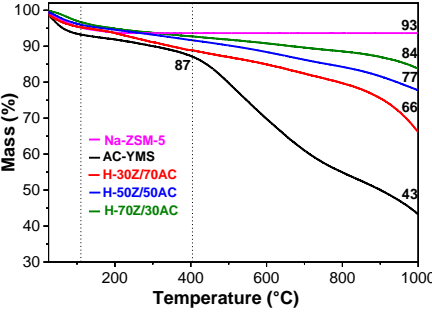


**Figure 5.** Thermogravimetric curves of activated carbon AC-YMS, Na-ZSM-5 zeolite and HAs prepared by physical mixture. Conditions: mass = 8 mg; heating rate = 10°C min<sup>-1</sup>, N<sub>2</sub> flow rate = 50 mL min<sup>-1</sup>.

The first stage of mass loss, around 110°C, is attributed to the desorption of adsorbed water and it is observed for all materials. Subsequently, the Na-ZSM-5 zeolite stands out for its thermal stability, remaining practically unchanged up to 1000°C. On the other hand, the activated carbon AC-YMS suffers significant decomposition from 405°C until 1000°C.

The incorporation of Na-ZSM-5 in the hybrids confers greater thermal stability compared to AC-YMS. After heating to 1000°C, the hybrids H-30Z/70AC, H-50Z/50AC, and H-70Z/30AC retain high percentages of residual mass (66%, 77%, and 84%, respectively), demonstrating a direct

 $<sup>{}^{</sup>b}S_{micro}$ , micropore surface area calculated by the Dubinin-Radushkevich method;

<sup>&</sup>lt;sup>c</sup> Pore volume calculated by NLDFT method assuming slit pore model.



dependence on the hybrid composition. In other words, a higher activated carbon content in the structure of the hybrid material leads to a greater mass loss at elevated temperatures. Up to 200°C, the temperature of the initial pre-adsorption treatment, all materials demonstrate good thermal stability, with mass losses of less than 10%.

#### CO<sub>2</sub> adsorption study by TG

Figure 6 presents the graphs of the  $CO_2$  capture curves for the activated carbon, zeolite and the HAs. It is observed that the activated carbon exhibits a significantly higher  $CO_2$  capture capacity (9.5  $\pm$  0.05%) compared to the zeolite (3.1  $\pm$  0.05%). Additionally, the  $N_2$  adsorption in Na-ZSM-5 during the process is higher than that of the activated carbon. These intrinsic characteristics of the constituent materials tend to influence the capture capacity of the hybrids depending on their composition.

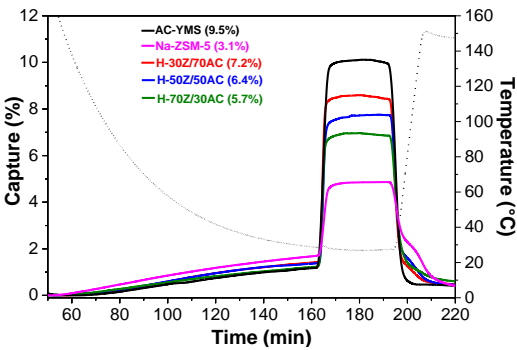


**Figure 6** CO<sub>2</sub> adsorption curves by TSA of the activated carbon AC-YMS, zeolite Na-ZSM-5 and Hybrid Adsorbents (HA). Conditions: P = 1 bar, T = 30°C e F = 100 mL min<sup>-1</sup> (50% CO<sub>2</sub> + 50% N<sub>2</sub>).

The curves obtained in the study of the  $CO_2$  adsorption-desorption capacities of the HAs are shown in Figure 6. During adsorption, H-30Z/70AC demonstrated a capacity of approximately  $7.2 \pm 0.05\%$ , evidencing that a larger proportion of activated carbon in the HA results in greater  $CO_2$  capture in the TSA process evaluated by thermogravimetric balance. The analysis of the Figure 6 reveals that the superior performance in  $CO_2$  capture in the hybrid materials is directly correlated with the activated carbon content. These results are consistent with the comparison of the  $CO_2$  capture curves of the precursor materials, given that activated carbon has a higher  $CO_2$  capture capacity than zeolite, and its incorporation into hybrid materials leads to an increase in their capture capacity.

Figure 7 illustrates the equilibrium curves for  $CO_2$  adsorption capacity performance of the HAs. Analysis of the graphs revealed that the H-30Z/70AC, H-50Z/50AC, and H-70Z/30AC adsorbents reached the equilibrium after near 5 min and exhibited  $CO_2$  adsorption capacities of 71.67 mg  $g^{-1}$ , 63.52 mg  $g^{-1}$ , and 57.28 mg  $g^{-1}$ , respectively. For  $N_2$  adsorption (Figure 6), the obtained values for the same HAs



were 14.32 mg g<sup>-1</sup>, 13.84 mg g<sup>-1</sup>, and 12.37 mg g<sup>-1</sup>, respectively. As a result, the calculated  $CO_2/N_2$  selectivities were 5.0 (H-70Z/30AC), 4.6 (H-50Z/50AC), and 4.6 (H-30Z/70AC), respectively.

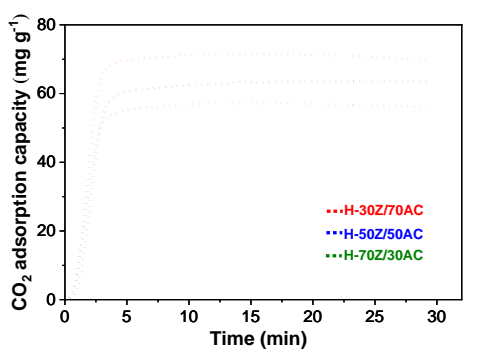


Figure 7.  $CO_2$  adsorption capacity ( $Q_{CO_2}$ ) of the HAs as a function of time.

Generally, both carbon dioxide and nitrogen adsorption on activated carbons and zeolites are recognized in the literature as governed by physisorption, since for TSA applications a fast adsorption and desorption kinetics is required (21). The results shown in Table 2 suggest that the proportions of AC-YMS and Na-ZSM-5 in the HAs influence the CO<sub>2</sub> adsorption performance at low pressures.

**Table 2.**  $CO_2$  adsorption capacities of the precursors and HAs. Conditions: P = 1 bar, T = 30°C and F = 100 mL min-1 (50%  $CO_2 + 50$ %  $N_2$ ).

Sample	Qco2 a (mg g-1)	Q <sub>N2</sub> b (mg g <sup>-1</sup> )	Qco2/Q <sub>N2</sub>
Na-ZSM-5	31.62	17.05	1.9
AC-YMS	85.88	11.48	7.4
H-30Z/70AC	71.67	14.32	5.0
H-50Z/50AC	63.52	13.84	4.6
H-70Z/30AC	57.28	12.37	4.6

<sup>&</sup>lt;sup>a</sup> Q<sub>CO2</sub> is the carbon dioxide capture capacity.

Consistent with what was previously stated, a higher concentration of activated carbon in the obtained HAs enhances the  $CO_2$  capture capacity. Nevertheless, an increase in  $N_2$  adsorption is also observed as the proportion of AC-YMS increases.

#### Conclusions

It was observed that the incorporation of AC-YMS activated carbon considerably modified the zeolite crystalline structure in the HAs. The materials exhibit a crystalline profile with the typical peaks of the zeolitic structure, originating from the mixing method employed, with the most pronounced effect observed in H-30Z/70AC. The SEM analyses demonstrated the influence of the

<sup>&</sup>lt;sup>b</sup> Q<sub>N2</sub> is the nitrogen capture capacity.



composition on the morphology of the HAs. In H-50Z/50AC, an interconnection between the Na-ZSM-5 crystals and the AC-YMS was observed, without a clear major phase. Differently, H-70Z/30AC was characterized by an activated carbon matrix heterogeneously and abundantly involving the ZSM-5 crystals. In contrast, H-30Z/70AC presented a structure where hexagonal polyhedral Na-ZSM-5 crystals predominated, with the activated carbon dispersed in small quantities around them.

Thermogravimetric analysis of the HAs demonstrated that, up to 200°C, the temperature of the initial pre-adsorption treatment, the three materials exhibit good thermal stability, with mass losses of less than 10%. It was also observed that a higher activated carbon content in the material composition leads to greater mass loss at higher temperatures.

The H-30Z/70AC, H-50Z/50AC, and H-70Z/30AC adsorbents exhibited  $CO_2$  adsorption capacities of 71.67 mg g<sup>-1</sup>, 63.52 mg g<sup>-1</sup>, and 57.28 mg g<sup>-1</sup>, respectively, demonstrating a positive correlation between the concentration of activated carbon in the HAs and the  $CO_2$  capture capacity. The results of the adsorption capacity performance allowed us to determine that the  $CO_2/N_2$  selectivity were 5.0 (H-70Z/30AC) and 4.6 for (H-50Z/50AC) and (H-30Z/70AC).

## **Acknowledgements**

J. Arce-Castro acknowledges CAPES for the scholarship granted. The authors also acknowledge the projects CATSUS-H2 (CNPq, Process 405869/2022-3), USINA (FINEP, Process 0057/21), FGTL (FINEP, Process 2435/22) and ESA-CO2 (FINEP, Process 2427/22)

## References

- 1. M.N. Anwar; A Fayyaz; N.F. Sohail; M.F. Khokhar; M. Baqar; W.D. Khan; K. Rasool; M. Rehan; A.S. Nizami, *J. Environ. Manage.* **2018**, 226, 131-144.
- M. Li, R. Xiao, Fuel Process. Technol., 2019, 186, 35-39
- T Watari, BC McLellan, D Giurco, E Dominish, E Yamasue, K Nansai. Resour. Conserv. Recycl., 2019, 148, 91-103.
- D. Gielen; F. Boshell; D. Saygin; M.D. Bazilian; N. Wagner; R. Gorini, Energy Strategy Rev., 2019, 24, 38-50.
- P.B. Ramos; A. Mamaní; M. Erans; F. Jerez; M. F. Ponce; M.F. Sardella, A. Amaya Arencibia; M.A. Bavio; E.S. Sanz-Pérez, R. Sanz, R. *Energy & Fuels*, 2024, 38,7, 6102-6115.
- A. Pereira; A.F. Ferreira; A. Rodrigues; A. M. Ribeiro;
   M.J. Regufe, *Chem. Eng. J.*, 2022, 450, 138197.
- 7. S.I. Gnani Peer Mohamed; S. Ismail; A. El-Harairy; M. Bavarian; S. Nejati. *ACS Appl. Eng. Mater.*, **2024**, *2*,7, 1743-1747.



- 8. L. Qiao; D. Fu, J. Environ. Chem. Eng., 2025, 13,1, 115218.
- S. Kundu; T. Khandaker; M.A.A.M. Anik; M.K. Hasan;
   P.K. Dhar; S.K. Dutta; M.A. Latif; M.S. Hossain, RSC Adv, 2024, 14,40, 29693-29736.
- 10. N.L. Ho; J. Perez-Pellitero; F. Porcheron; R.J.M. Pellenq, *J. Phys. Chem. C.*, **2012**, *116*, 5, 3600-3607.
- 11. A. Masala, J.G. Vitillo; G. Mondino; G. Martra; R. Blom, R. C.A. Grande; S. Bordiga, *Ind. Eng. Chem. Res*, **2017**, *56*, *30*, 8485-8498.
- 12. Q. Zhao; F. Wu; K. Xie; R. Singh; J. Zhao; P. Xiao; P.A. Webley, *Chem. Eng. J.*, **2018**, *336*, 659-668.
- 13. Y. Gomez-Rueda, B. Verougstraete, C. Ranga, E. Perez-Botella, F. Reniers, J. F. Denayer, *Chem. Eng. J.*, **2022.** *446*, 137345.
- 14. K. Wu, S. Deng, S. Li, R. Zhao, X. Yuan, L. Zhao, *Carbon Capture Sci. Technol.*, **2022**. 2, 100035.
- A. Das, S. D. Peu, M. S. Hossain, M. M. A. Nahid, F. R. B. Karim, H. Chowdhury, M. H. Porag, D. B. P. Argha, S. Saha, A. R. M. T. Islam, M. M. Salah, Shaker, A. *Heliyon*, 2023. 9,12, e22341.
- F. O. Erdogan, Int. J. Environ. Anal. Chem., 2022, 102,19,7523-7541.
- 17. M.B. dos Santos, K.C. Vianna, H.O. Pastore, H.M. Andrade, A.J. Mascarenhas. Micropor. Mesopor. Mat. **2020**, *306*, 110413.
- 18. J. Hao, J. Bai, X. Wang, Y. Wang, Q. Guo, Y. Yang, Z. Jiupeng, C. Caixia, Y.S. Li, *Nanoscale Adv.*, **2021**, *3*, *3*, 738-746.
- 19. Z. Heiderinejad, M.H. Dehghani, M. Heidari, G. Javedan, I. Ali, M. Sillanpaa, *Environ. Chem. Lett.*, **2020**, *18*, 393-415.
- 20. M. Thommes, K. A. Cychosz, *Adsorption*, **2014**, *20*,2–3, 233-250.
- 21. R. González-Olmos, A. Gutierrez-Ortega, J. Sempere, R. Nomen, *J. CO<sub>2</sub> Utilization*, **2022**, *55*, 101791.